PAPER 2002-296

Data sufficiency for reservoir development decision-making in the presence of uncertainty

Sanjay Srinivasan, University of Calgary

C. V. Deutsch, University of Alberta

This paper is to be presented at the Petroleum Society's Canadian International Petroleum Conference 2002, Calgary, Alberta, Canada, June 11 – 13, 2002. Discussion of this paper is invited and may be presented at the meeting if filed in writing with the technical program chairman prior to the conclusion of the meeting. This paper and any discussion filed will be considered for publication in Petroleum Society journals.

Abstract

Uncertainty stemming from the sparse information available to model a reservoir and from the lack of complete knowledge about the flow processes in the reservoir is an inescapable aspect of reservoir modeling. Methodologies for assessing that uncertainty and techniques for incorporating that uncertainty in exploration and development decisions are crucial for successful management of assets. This paper presents a reservoir modeling case study demonstrating typical steps in the exploration of a reservoir and aspects of uncertainty assessment using geostatistical techniques. The viability of using simple, easy to use connectivity measures for assessing the productivity of candidate well locations prior to actually drilling the well is explored. A Bayesian methodology to incorporate seismic data in reservoir models is presented.

Introduction

The true distribution of facies, porosity and permeability in a petroleum reservoir cannot be uniquely determined using the information from a few widely spaced wells. Geological uncertainty in the form of local uncertainty - the uncertainty in an attribute value at any given location in the reservoir and joint uncertainty - uncertainty in the connectivity characteristics of the reservoir are an inescapable aspect of reservoir modeling. Decisions such as collection of additional data for improved reservoir delineation, location of additional wells for reserves depletion and implementation of improved oil recovery would have to be based on an assessment of geological and reservoir response uncertainty and the potential impact of additional data on that uncertainty.

This paper presents a methodology for integrating seismic and well data in order to develop stochastic representations of the reservoir. Decisions pertaining to reservoir development in the presence of uncertainty are evaluated. Since geostatistics provides a framework for integrating data from diverse sources and for assessing geologic uncertainty, the issue of data sufficiency and the worth of additional reservoir specific information will be examined using geostatistical tools. The modeling methodology and techniques for assessment of uncertainty are demonstrated on the Stanford V reservoir[1], a synthetic data set developed specifically to test the accuracy of reservoir characterization techniques.

Due to the nature of the interaction between reservoir rocks and seismic waves, there is an inherent imprecision in seismic data as it

pertains to reservoir average porosity and lithofacies proportions. Stochastic modeling techniques have to account for this imprecision. Numerous authors[2-5] have proposed techniques for integration of seismic data accounting for scale and precision issues. Most conventional geostatistical techniques account for the imprecise relationship between seismic and the primary variable of interest e.g. porosity by including the seismic data as a secondary variable. The cross-correlation between the primary and secondary variable is included in the spatial interpolation scheme (kriging) in order to arrive at the estimate of primary variable at an unsampled location. This paper presents a Bayesian scheme for updating the prior conditional probability of observing the pay facies at a location in the reservoir into a posterior probability incorporating seismic data. The lithofacies models resulting after the application of the technique appear geologically plausible and the procedure is extremely fast.

Reservoir development decision-making in the presence of uncertainty is an important aspect of modern reservoir management. Ranking of reservoir model in order to facilitate evaluation of uncertainty in reservoir performance has been proposed by some researchers[6,7]. The use of reservoir quality maps[8] for optimally locating development wells has also been proposed. The development of such a quality map requires repeated runs of a flow simulator and is consequently computationally expensive. This paper evaluates the use of static reservoir connectivity measures for optimal location of wells. More emphasis is placed on understanding the influence of data on reservoir development decisions and assessing the accuracy of the reservoir models resulting from the proposed data integration methodology.

The methodology for data integration and uncertainty assessment is demonstrated using a synthetic reservoir model that is described next.

Stanford V Reservoir

The Stanford V reservoir[1] is a synthetic multi-layered fluvial reservoir. The synthetic model was developed so as to facilitate extensive testing of new reservoir characterization algorithms. The synthetic data set is complete with:

- Layer surfaces: Top and bottom surface of each layer
- Lithofacies indicators
- Petrophysical properties: porosity (ϕ), permeability (k), rock density (ρ) and wave velocity (v)
- Seismic data: two-way travel time, impedance

The layer geometries were developed using stochastic simulation techniques. Object-based lithofacies models were developed for each layer and then transformed to reflect the actual layer geometries. The reservoir model was populated with petrophysical properties such as porosity and permeability obtained using stochastic simulation techniques. Rock density was obtained as an weighted function of matrix and fluid densities:

$$\rho(\mathbf{u}) = \phi(\mathbf{u}) \cdot \rho_{fluid} + [1 - \phi(\mathbf{u})] \cdot \rho_{matrix}(\mathbf{u})$$

where ρ_{fluid} is fluid density

$\rho_{matrix}(\mathbf{u})$ is mineral density

The velocity of seismic wave in channel, crevasse-splays and mudstone were calculated using regressions[1]. These regressions relate the velocity to the porosity of the rock and in some case to the density of the rock material. Seismic impedance is equal to the product of rock density and velocity. In order to mimic the impedance obtained from a seismic inversion procedure, a frequency domain Born filter was applied on the high-resolution impedance. A local Backus average with vertical sliding window was applied to smooth out thin layers and to mimic the resolution of field-gathered seismic data. Finally, normal ray tracing theory is applied to compute the seismic velocity and the two-way travel time to layer surfaces.

In this work, the Stanford V data set is utilized to demonstrate the evolution of the reservoir model over the course of reservoir exploration. The impact of decisions made on the basis of these reservoir models is assessed against the true response obtained on the reference Stanford V reservoir data set.

Well placement using seismic

The acquired seismic data is interpreted using knowledge about the specific geological depositional model for the reservoir in order to arrive at an integrated reservoir model. In the absence of any other reservoir specific information, decisions pertaining to exploration of the reservoir such as location of exploratory wells have to be based on this preliminary reservoir model. Factors such as the extent of pay, the average porosity as well as the connectivity of permeability in the region influence well placement decisions.

Seismic impedance is inversely proportional to the porosity and to the proportion of pay facies at a location in the reservoir. Figure 1 shows slices through the 3-D seismic impedance cube and the impressions of the fluvial channels are faintly visible. The vertical and lateral resolution of the seismic data is determined by the characteristics of the seismic wavelet, which in turn is influenced, by the characteristics of the seismic acquisition devices. In this synthetic example, the precision of the seismic impedance data are influenced by the characteristics of the Born filter used for synthesizing the seismic impedance signature.

The connectivity in different regions of the reservoir has to be assessed prior to deciding on candidate locations for exploratory drilling. The concept of geobodies[9] can be used to assess the connectivity to wells located at different locations within the reservoir. The reservoir is first coded into pay or non-pay regions using a suitable impedance threshold. A cubic template is defined and adjacent voxels that jointly exceed the set threshold are further coded as being part of a common geobody. Figure 2 depicts the distribution of the main geobodies in the reservoir. The size of the largest geobody connected to potential well locations can be used to rank these locations. The five locations picked for exploratory drilling are shown in Figure 3. The size of the largest geobody connected to each of these locations is 2500, indicating that a mass of fifteen hundred voxels jointly below the impedance threshold are present in the vicinity of the well.

The production profiles at the selected well locations were simulated using the exhaustive data available for the reference reservoir. These simulated profiles shown in Figure 4 are indicative of the production potential of the wells and have been simulated assuming nominal fluid and reservoir properties summarized in Table 1. In order to render the case study from interesting from a decision-making standpoint, the economic sustained oil flow rate is specified to be 4000 STB/day. Any well that is unable to sustain that flow rate for the test period is deemed uneconomical and not contributing to the booked reserves. Based on the flow simulation results in Figure 4, the drilling rate for the initial exploration phase is 80%.

The wells drilled during the initial exploratory phase provide valuable reservoir specific information that should be utilized to update the reservoir model. The well information has to be integrated with the seismic information accounting for the difference in scale and precision of the different data, a task particularly suited for geostatistics.

Stochastic reservoir modeling incorporating seismic data

Figure 5 depicts the histogram of porosity values recorded along the wells. The existence of two distinct porosity populations is evident. The calibration scatterplot between co-located seismic impedance and porosity values, Figure 6,

confirms the existence of two porosity populations. The figure further demonstrates that the seismic impedance data can be utilized to discriminate between the pay/non-pay porosity populations. A multi-step reservoir modeling procedure was adopted:

Step1: Indicator modeling of facies distribution in reservoirs.

Step2: Modeling of porosity based on prior modeling of facies.

Step3: Permeability modeling conditioned to distribution of facies and porosity in the reservoir.

The facies data observed along the well trajectories are first indicator coded:

$$I(\mathbf{u}) = \begin{cases} 1 \text{ if } \mathbf{u} \in \text{pay facies} \\ 0 \text{ if not} \end{cases}$$

where the mudstone, crevasse-splays as well as the levies are assumed to constitute the non-pay facies while the channels and the channel margins constitute the pay facies. The assignment of lithologies to pay and non-pay facies is based on a porosity cut-off. The corresponding histogram of porosity in the pay and non-pay facies is shown in Figure 6.

The probability of a particular unsampled location within the reservoir belonging to a pay/non-pay facies conditioned to the available data in the vicinity of the estimation point is given by indicator kriging[10]:

$$I^*(\mathbf{u}) = \text{Prob}\{u \in \text{pay} \mid n \text{ data}\} = p(\mathbf{u}) + \sum_{\alpha=1}^{n(\mathbf{u})} \lambda(\mathbf{u}_\alpha) \cdot [I(\mathbf{u}_\alpha) - p(\mathbf{u}_\alpha)] \quad (1)$$

$n(\mathbf{u})$ represents the data in the neighbourhood of the location $\mathbf{u}$, $p(\mathbf{u})$ represents the prior probability of pay facies at location $\mathbf{u}$ and $p(\mathbf{u}_\alpha)$ is the prior probability at data location $\mathbf{u}_\alpha, \alpha = 1,...,n(\mathbf{u})$. The n weights $\lambda(\mathbf{u}_\alpha)$ are obtained by solving a kriging system:

$$\sum_{\beta=1}^{n(\mathbf{u})} \lambda(\mathbf{u}_\beta) \cdot C_I(\mathbf{h}_{\alpha\beta}) = C_I(\mathbf{h}_{\alpha 0}), \quad \forall \alpha = 1,...,n(\mathbf{u}) \quad (2)$$

$C_I(\mathbf{h}_{\alpha\beta})$ is the indicator covariance between two data locations $\mathbf{u}_\alpha$ and $\mathbf{u}_\beta$, $C_I(\mathbf{h}_{\alpha 0})$ is the indicator covariance between the data at $\mathbf{u}_\alpha$ and the estimation point $\mathbf{u}$. The requisite covariances are inferred using the available data The indicator covariances measure the joint probability that two locations separated by a lag $\mathbf{h}$ will be in the pay facies i.e. they describe the spatial variability of the reservoir.

Expression (1) is the updated probability that the location u will be in the pay facies. The simulated facies at that location can be obtained by performing a Monte Carlo draw from the updated probability distribution. In the sequential simulation framework, covariance reproduction is ensured by assimilating this simulated category into the conditioning database and proceeding to the next node along a random path. Covariance reproduction is analogous to stipulating that the resultant reservoir models exhibit the correct pattern of spatial variability. The indicator simulation procedure comprises of the following steps:

1. Construct the conditional probability density function (*cpdf*) at location $\mathbf{u}$ using the surrounding conditioning data.
2. Draw a random number r
   if $r \le cpdf(\mathbf{u} \mid \text{n data})$ then
   $I^\ell(\mathbf{u}) \in \text{pay facies}$
   else
   $I^\ell(\mathbf{u}) \in \text{non pay facies}$
3. Add simulated $I^\ell(\mathbf{u})$ to the data set $n \to n+1$
4. Proceed to the next simulation node **u'**

Integrating seismic data

As seen in Figure 6, the seismic impedance data appears to discriminate between pay/non pay facies. In order to confirm this,

define the likelihood of seismic impedance given $\mathbf{u} \in$ pay as:

$$F(s \mid 1) = Prob\{S(\mathbf{u}) \le s \mid \mathbf{u} \in \text{pay}\} \quad (3)$$

where $S(\mathbf{u})$ is the impedance at location $\mathbf{u}$. Similarly:

$$F(s \mid 0) = Prob\{S(\mathbf{u}) \le s \mid \mathbf{u} \in \text{nonpay}\} \quad (4)$$

If $F(s \mid 1) \neq F(s \mid 0)$, then it can be concluded that the seismic impedance does indeed discriminate between pay and non-pay.

Figure 7 shows the quantile-quantile comparison of the two likelihood functions in expressions (3) and (4). The scatter of points deviates from the 45° line indicating that the two likelihood functions are indeed different, thereby implying that seismic impedance does indeed differentiate between pay/non-pay facies.

In order to integrate the available seismic data within a stochastic reservoir-modeling framework, it is necessary to evaluate the conditional probability:

$$Prob\{I(\mathbf{u}) = 1 \mid s(\mathbf{u}) \in [s_l, s_{l+1}]\}$$

Applying Bayes' theorem:

$$Prob\{A \mid B\} = \frac{Prob\{B \mid A\}}{Prob\{B\}} \cdot Prob\{A\} \quad (5)$$

the required conditional probability can be written as:

$$Prob\{I(\mathbf{u}) = 1 \mid s(\mathbf{u}) \in [s_l, s_{l+1}]\} = \frac{Prob\{s(\mathbf{u}) \in [s_l, s_{l+1}] \mid I(\mathbf{u}) = 1\}}{Prob\{s(\mathbf{u}) \in [s_l, s_{l+1}]\}} \cdot P\{I(\mathbf{u}) = 1\}$$

This simply amounts to:

$$Prob\{I(\mathbf{u}) = 1 \mid s(\mathbf{u}) \in [s_l, s_{l+1}]\} = \frac{F(s_{l+1} \mid 1) - F(s_l \mid 1)}{F(s_{l+1}) - F(s_l)} \cdot p(\mathbf{u}) \quad (6)$$

The Bayesian updating procedure therefore consists of locating the class l to which the seismic impedance value s($\mathbf{u}$) belongs and computing the conditional probability of the pay facies occurring using the expression (6). This conditional probability has to be merged with the kriging derived distribution in order to arrive at reservoir models that honor the facies information recorded at the wells, the seismic response and reflect the correct pattern of spatial variability.

Locally varying mean: The seismic derived $Prob\{I(\mathbf{u}) = 1 \mid s(\mathbf{u}) \in [s_l, s_{l+1}]\}$ can be identified with the locally varying proportion of pay facies in the reservoir. The kriging system is then rewritten as:

$$I^*(\mathbf{u}) = p_S(\mathbf{u}) + \sum_{\alpha=1}^{n(\mathbf{u})} \lambda_\alpha \cdot [I(\mathbf{u}_\alpha) - p_S(\mathbf{u}_\alpha)]$$

where $p_S(\mathbf{u})$ is the seismic derived probability in Expression (6).

Figure 8a shows the horizontal variograms inferred in the 60° azimuth and 150° azimuth directions based on the seismic impedance data and the model fit. At this stage of reservoir model development, inadequate well facies information is available in order to infer the variogram and hence is substituted by the exhaustively available seismic data. The vertical variogram is inferred using the abundantly available facies data along the well trajectories and is shown in Figure 8b. The salient variogram parameters are summarized in Table 2.

Figure 9 shows two XY slices through the resultant reservoir model. The simulated reservoir models were subjected to a histogram transformation procedure in order to ensure that the simulated models honour the target pay/non-pay proportions accurately. For comparison, the corresponding slices through the 3-D seismic impedance cube are shown in Figure 10. Sequential simulation is a stochastic procedure that gives rise to multiple such facies models of the reservoir, each honoring the well information as well as the seismically derived probability data.

Simulating the porosity field

The histograms of porosity corresponding to the pay and non-pay facies are shown in Figure 11. Due to the presence of two distinct porosity populations, stochastic

simulation of porosity corresponding to the two populations was carried out separately and finally the two porosity models were merged using the facies template modeled previously.

The locally varying mean porosity in the reservoir was calculated using a cubical spatial template comprising of 9 nodes. The locally varying mean porosity was calculated using:

$$\bar{\phi}(\mathbf{u}) = p(\mathbf{u}) \cdot \bar{\phi}_{pay} + \left(1 - p(\mathbf{u})\right) \cdot \bar{\phi}_{non-pay} \quad (7)$$

The use of locally varying means derived from the facies model helps ensure that there is consistency between the facies and the porosity models and pay regions previously identified have higher simulated porosity. Two separate sequential Gaussian simulations were performed using the conditioning data in pay and non-pay facies respectively. In Gaussian simulation, the kriging procedure utilizes the porosity values at data locations and yields an estimate for porosity at the simulation node and also the estimation variance. The weights λ_α are again obtained by solving the kriging system (Expression (2)). The estimated value and variance are identified with the mean and variance of a Gaussian conditional distribution. The simulated value of porosity at the unsampled location is obtained by performing a Monte Carlo draw. The simulated value is added to the conditioning data set and the simulation proceeds to the next location in the reservoir along a random path. Since sparse well information is available for inferring the horizontal porosity variograms, the variogram model summarized in Table 2 was utilized for the porosity simulation also.

Figure 12 shows a slice through the simulated porosity model for pay and non-pay facies and the final merged model. The higher porosity areas are aligned along the channel-like pay facies.

Simulating the permeability field

Figure 13 depicts the histogram of permeability values in pay and non-pay facies. The calibration scatter plot between porosity and permeability in the pay and non-pay facies are shown in Figure 14. The wide variation in permeability values in the pay-facies renders the correlation between porosity and permeability low. On the other hand, the correlation is high in the non-pay facies. In view of the permeability data observed in the wells, eparate Gaussian simulations of permeability in pay and non-pay facies were performed. The simulation of permeability in the pay facies was performed utilizing locally varying permeability means computed using a formulation similar to Expression (7).

Simulation of permeability at a location **u** in the non-pay facies was performed using the co-located porosity value $\phi_{sim}(\mathbf{u})$. The co-located porosity value was assumed to screen the influence of porosity values at all other locations on the estimate of permeability at **u**. In this type of Markov I model[11], the cross-covariance between the porosity and permeability random variables is derived from the auto-covariance model for permeability by scaling it using the correlation coefficient between porosity and permeability, i.e.

$$C_{\phi-k}(\mathbf{h}) = \rho_{\phi-k} \cdot C_k(\mathbf{h}) \quad (8)$$

$\rho_{\phi-k}$ is the correlation coefficient, 0.70 in this case, $C_k(\mathbf{h})$ is the permeability variogram model in Table 2.

Figure 15 shows slices through the merged permeability model. The consistency between the simulated facies, porosity and permeability model is evident.

Assessing uncertainty and locating wells

Stochastic simulation techniques yield multiple equally probable models of the reservoir. Each of these models honours all the available data and reflects the correct spatial variability as captured by the spatial covariance model. A total of ten lithofacies models were generated, each conditioned to the available seismic information. The locally varying mean porosities computed

on the basis of each facies model were utilized to generate a set of ten porosity and permeability models. Thus a total of hundred reservoir models were developed and these reflect the uncertainty due to sparse information.

A second set of candidate well locations was evaluated using the connectivity tools discussed earlier. The size of geobodies connecting to the well locations was calculated corresponding to each realization of the reservoir. The candidate locations were ranked on the basis of the mean size of the geobodies and the variance of the geobody size over the entire suite of reservoir models. The five well locations selected for the second phase of exploration are shown in Figure 16. The mean and variance of the geobody size at each candidate location as well as the coefficient of variation is summarized in Table 3. The production response at these candidate well locations was simulated using the exhaustive data and these are depicted in Figure 17. Stipulating that the sustained flowrate has to exceed 4000 STB/day for the well to be deemed a producer, the success rate in this case is 100%. More interestingly, the suite of reservoir models developed using geostatistical techniques can provide some insights into the uncertainty characteristics and the robustness of the modeling procedure.

Are geobodies useful tools for rapid assessment of uncertainty?

In order to answer this question, flow simulation was performed on the suite of reservoir models. The cumulative oil recovery over the production period was tabulated against the size of the geobody connected to a well location. Figure 18 is a calibration plot between the size of the geobody and the cumulative oil recovery. The correlation coefficient is a modest 0.47. Scenarios where a well is adjacent to a large geobody mass but not within the geobody itself may result in the well having a high cumulative production even with low geobody size. Counting such extreme cases out, the correlation coefficient improves to 0.67. Regardless of the actual value of the correlation coefficient, the relatively high success rate encountered during the exploratory drilling suggest that even a coarse measure of connectivity would suffice for rapid assessment of uncertainty prior to placement of exploratory wells.

Is detailed modeling of reservoir attributes necessary or is a 3D seismic cube sufficient for locating wells?

The candidate well locations selected for the second phase of exploration were based on an assessment of uncertainty using the suite of models. The size of geobodies connected to these well locations computed on the basis of the seismic impedance model at four of these locations is zero indicating that these locations would not have been proposed as candidate locations if the decision had been based on seismic impedance data only. The additional effort expended for assessment of geologic uncertainty and the calibration approach for integrating seismic data does result in identification of productive well locations that would have been otherwise bypassed.

Discussions and Conclusions

The paper presents a methodology for geostatistical modeling of reservoir integrating seismic impedance and well information. The methodology is demonstrated on a synthetic yet realistic reservoir example developed specifically for the purpose of testing geostatistical algorithms. The case study tracks the typical steps followed during the exploratory phase of a reservoir. Some of the salient conclusions of the paper are:

- Assessment of uncertainty and incorporating that uncertainty into reservoir development decisions is an essential aspect of modern reservoir management.
- Calibrating the information present in seismic data and then performing a probabilistic integration of that information results in accurate models that can yield reliable answers for questions such as - Where to locate wells? How much data is sufficient for

reservoir modeling? How to manage the reservoir?

- Rapid assessment of uncertainty prior to implementing reservoir development decisions is possible by utilizing coarse measures of reservoir connectivity such as geobodies. Improved correlation between geobody characteristics and reservoir flow response is possible by defining optimal thresholds for calculating geobodies. Development of procedures for determining such thresholds is necessary.

Acknowledgements

The research was funded through an operating grant from COURSE (Coordination of University Research for Synergy and Effectiveness).

References

1. Mao, S.: *Multiple layer surface mapping with seismic data and well data*, Ph.D. thesis, Stanford University, 1999.
2. Deutsch, C.V., Srinivasan, S. and Mo, Y.: "Geostatistical Reservoir Modeling Accounting for Scale and Precision of Seismic Data", SPE 36497, SPE Annual Technical Conference and Exhibition, Denver, 1996.
3. Doyen, P.: "Porosity from seismic data: A geostatistical approach", Geophysics Vol. 53, No. 10, 1988, pp 1263-1275.
4. Behrens, R.A. and Tran, T.T.: "Incorporating seismic data of intermediate vertical resolution into 3D models", SPE 49143, SPE Annual Technical Conference and Exhibition, New Orleans, 1998.
5. Bortoli, L.J., Alabert, F., Haas, A. and Journel, A.G.: "Constraining stochastic images to seismic data", *Proceedings of the International Geostatistical Congress*, Troia 1992, P. Soares (editor), Kluwer, Dortrecht.
6. Deutsch, C.V. and Srinivasan, S.: "Improved reservoir management through ranking stochastic reservoir models", SPE 35411, SPE/DOE Improved Oil Recovery Symposium, Tulsa, 1996.
7. Ballin, P.R., Aziz, K. and Journel, A.G. "Quantifying the impact of geological uncertainty on reservoir performance forecast, SPE 25238, 1993.
8. Cruz, P.S., Horne, R.N. and C. V. Deutsch, "The Quality Map: A Tool for Reservoir Uncertainty Quantification and Decision Making,", SPE ATCE, October 3-6, 1999, Houston, TX.
9. Deutsch, C.V., "FORTRAN Programs for Calculating Connectivity of 3-D Numerical Models and for Ranking Multiple Realizations," Computers & Geosciences, v.24, no.1, pp. 69-76 1998.
10. Deutsch, C.V. and Journel, A.G.: *GSLIB - Geostatistical software library and users guide*. Oxford University press, 1998.
11. Journel, A.G.: "Markov models for cross covariances", Mathematical Geology, 31(8), pp 955-963, 1999.

Grid Dimension	120x120x10
Block Size (ft)	200x200x3.3
Well P_{wf} (psia)	400
Oil viscosity (cps)	1.0
P_i (psia)	2000
B_{oi} (bbl/STB)	1.05
Oil density (lb/ft^3)	26.72

Table 1: Reservoir flow simulation parameters.

Nugget Effect	0.18
Structure 1:	
Shape	Spherical
Sill	0.63
Aniostropy direction	60^o
Max. Range	19
Min. Range	17
Vertical Range	3.5
Structure 2:	
Shape	Spherical
Sill	0.19
Aniostropy direction	60^o
Max. Range	65
Min. Range	17
Vertical Range	4.0

Table 2: Variogram parameters used in stochastic simulations

Well #	Mean Geobody	Std. Dev. of size
1	165.41	62.19
2	50.41	21.64
3	34.01	16.60
4	56.98	22.55
5	50.92	22.38

Table 3: Mean size of geobody and the standard deviation of size connected to well locations.

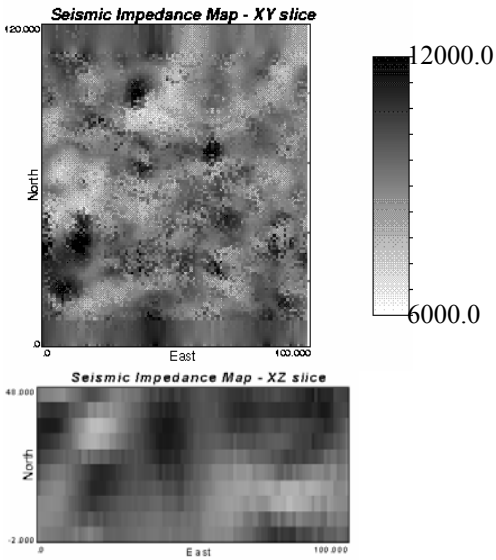

Figure 1: XY and XZ slices through the seismic impedance cube

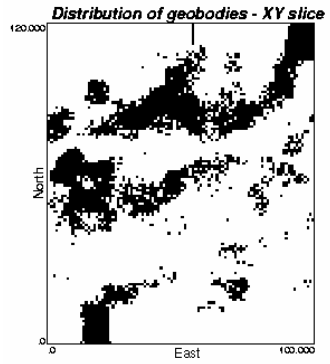

Figure 2: Distribution of geobodies on an XY slice through the reservoir.

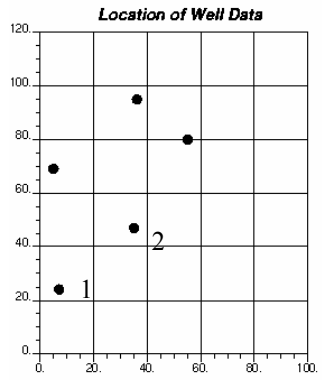

Figure 3: Location of vertical wells based on the analysis of impedance data.

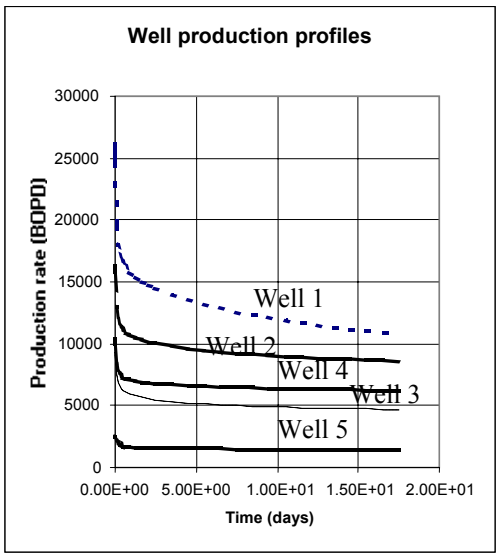

Figure 4: Well production profiles corresponding to well locations in Figure 3.

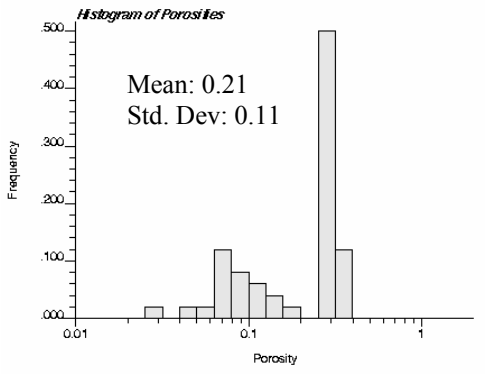

Figure 5: Histogram of porosities based on well data.

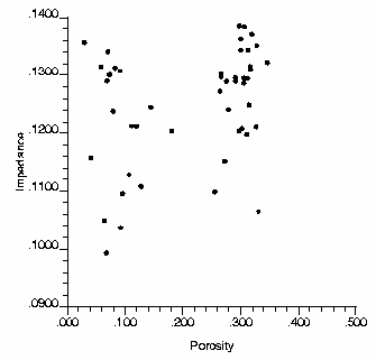

Figure 6: Calibration scatterplot between porosity and seismic impedance.

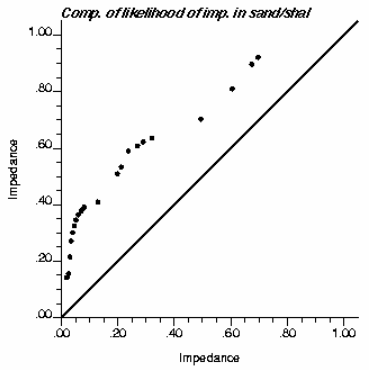

Figure 7: Comparison of likelihood of seismic impedance in pay versus non-pay.

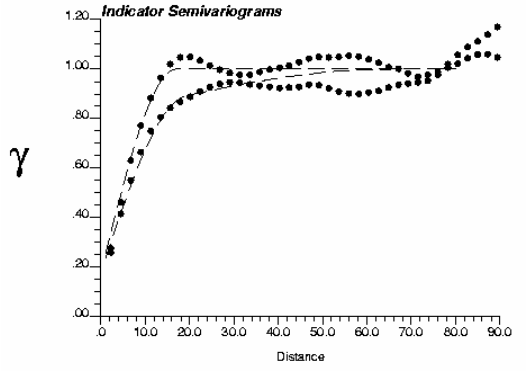

(a)

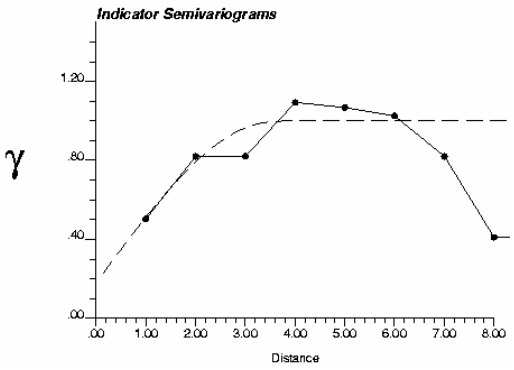

(b)

Figure 8: a) Variograms inferred from impedance data in the 60^o and 150^o direction. b) Variogram in the vertical direction inferred from well data.

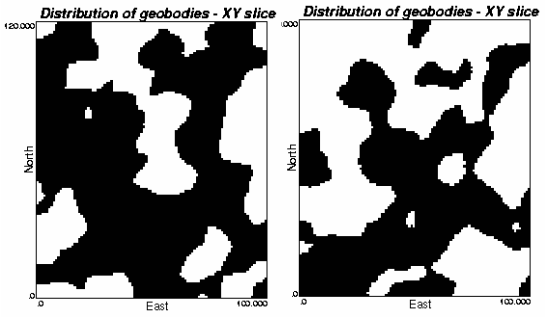

Figure 9: Two slices through the simulated lithofacies model.

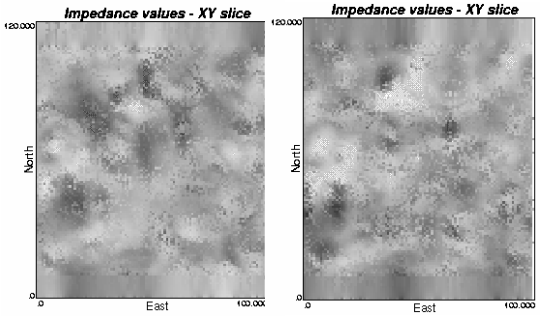

Figure 10: Corresponding two slices through the seismic impedance cube.

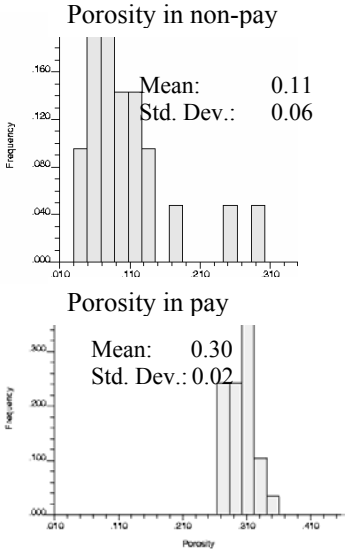

Figure 11: Histogram of porosity in non-pay and pay.

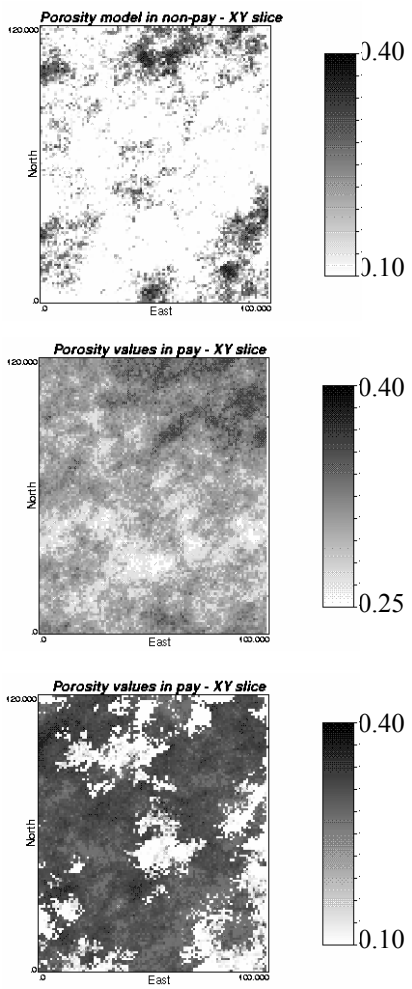

Figure 12: Porosity slice from the model in non-pay, pay and final merged model.

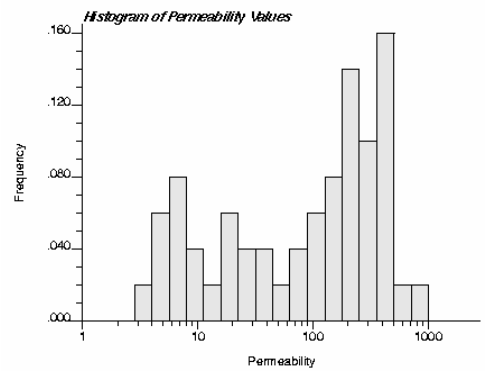

Figure 13: Histogram of permeability measured along wells.

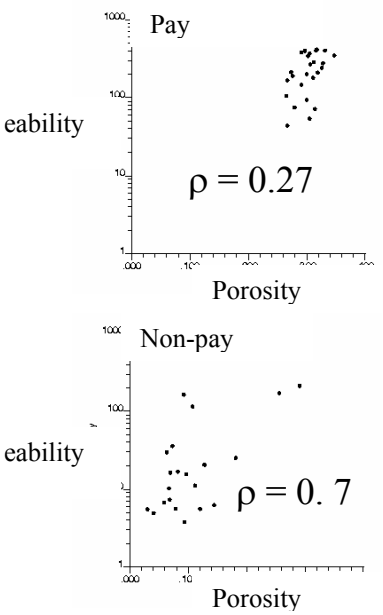

Figure 14: Calibration scatterplot between porosity and permeability in pay and non-pay.

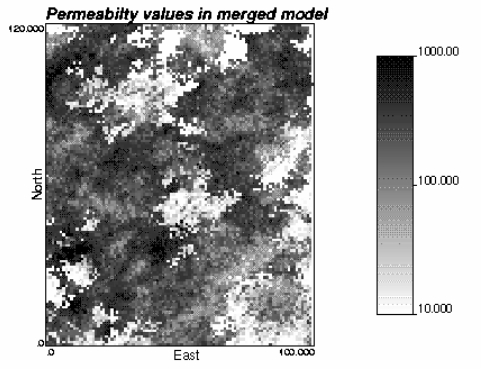

Figure 15: A slice through one realization of the merged permeability model.

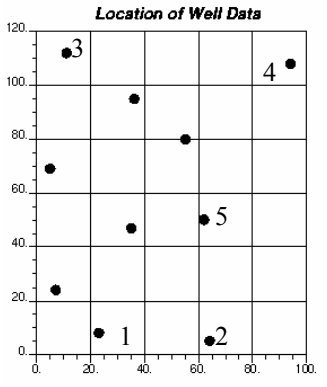

Figure 16: Location of additional vertical wells based on the suite of geostatistical simulations.

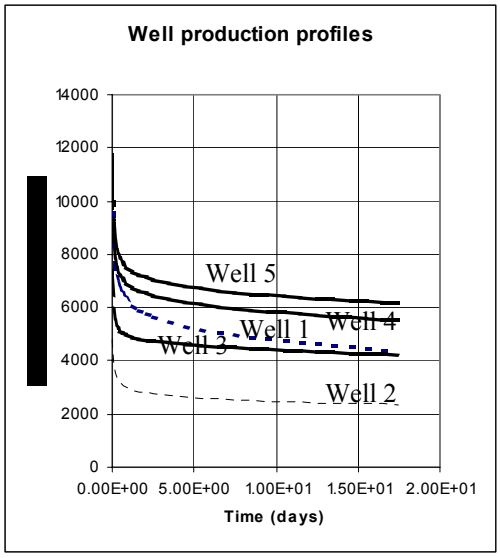

Figure 17: Well production profile corresponding to the additional wells.

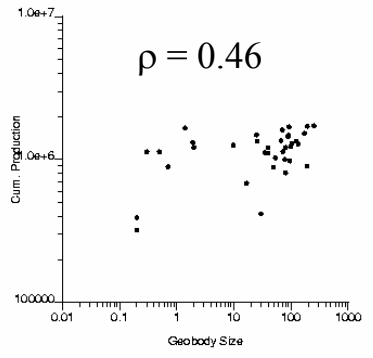

Figure 17: Calibration plot between geobody size and cum. production for the test period.